Brain-Computer-Spinal Interface Restores Upper Limb Function After Spinal Cord Injury

Soshi Samejima, Abed Khorasani, Vaishnavi Ranganathan, Jared Nakahara, Nicholas M. Tolley, Adrien Boissenin, Vahid Shalchyan, Mohammad Reza Daliri, Joshua R. Smith, *Fellow, IEEE*, and Chet T. Moritz

***Abstract*— Brain-computer interfaces (BCIs) are an emerging strategy for spinal cord injury (SCI) intervention that may be used to reanimate paralyzed limbs. This approach requires decoding movement intention from the brain to control movement-evoking stimulation. Common decoding methods use spike-sorting and require frequent calibration and high computational complexity. Furthermore, most applications of closed-loop stimulation act on peripheral nerves or muscles, resulting in rapid muscle fatigue. Here we show that a local field potential-based BCI can control spinal stimulation and improve forelimb function in rats with cervical SCI. We decoded forelimb movement via multi-channel local field potentials in the sensorimotor cortex using a canonical correlation analysis algorithm. We then used this decoded signal to trigger epidural spinal stimulation and restore forelimb movement. Finally, we implemented this closed-loop algorithm in a miniaturized onboard computing platform. This Brain-Computer-Spinal Interface (BCSI) utilized recording and stimulation approaches already used in separate human applications. Our goal was to demonstrate a potential neuroprosthetic intervention to improve function after upper extremity paralysis.**

***Index Terms*— Brain–computer interface, cervical spinal cord injury, local field potentials, epidural stimulation, upper limb function.**

Manuscript received January 8, 2021; revised May 8, 2021 and June 10, 2021; accepted June 14, 2021. Date of publication June 17, 2021; date of current version June 30, 2021. This work was supported in part by the Center for Neurotechnology, a National Science Foundation-Engineering Research Center under Grant EEC-1028725, in part by the Allen Distinguished Investigator Grant from the Paul G. Allen Family Foundation, in part by the Christopher and Dana Reeve Foundation International SCI Consortium, in part by the University of Washington Institute for Neuroengineering established by the Washington Research Foundation, and in part by the Washington State Spinal Cord Injury Consortium. *(Soshi Samejima and Abed Khorasani contributed equally to this work.) (Corresponding author: Chet T. Moritz.)*

Soshi Samejima is with the Department of Electrical and Computer Engineering, University of Washington (UW), Seattle, WA 98195 USA (e-mail: soshis@uw.edu).

Abed Khorasani was with the Department of Rehabilitation Medicine, UW, Seattle, WA 98195 USA. He is now with the Neuroscience Research Center, Institute of Neuropharmacology, Kerman University of Medical Sciences, Kerman 76169-13555, Iran.

Vaishnavi Ranganathan is with the Microsoft Research, Redmond, WA 98052 USA.

Jared Nakahara is with the Department of Electrical and Computer Engineering, University of Washington, Seattle, WA 98195 USA.

Nicholas M. Tolley and Adrien Boissenin were with the Department of Rehabilitation Medicine, University of Washington, Seattle, WA 98195 USA.

Vahid Shalchyan and Mohammad Reza Daliri are with the Neuroscience and Neuroengineering Research Laboratory, Biomedical Engineering Department, School of Electrical Engineering, Iran University of Science and Technology (IUST), Tehran 13114-16846, Iran.

Joshua R. Smith is with the Department of Electrical and Computer Engineering, University of Washington, Seattle, WA 98195 USA, and also with the Department of Computer Science and Engineering, University of Washington, Seattle, WA 98195 USA.

Chet T. Moritz is with the Department of Electrical and Computer Engineering, University of Washington, Seattle, WA 98195 USA, also with the Department of Rehabilitation Medicine, University of Washington, Seattle, WA 98195 USA, also with the Department of Physiology and Biophysics, University of Washington, Seattle, WA 98195 USA, and also with the Center for Neurotechnology, University of Washington, Seattle, WA 98105 USA (e-mail: ctmoritz@uw.edu).

This article has supplementary downloadable material available at https://doi.org/10.1109/TNSRE.2021.3090269, provided by the authors.

Digital Object Identifier 10.1109/TNSRE.2021.3090269

I. Introduction

SPINAL cord injury (SCI) results in lifelong disability due to disrupted neural connections between the brain and spinal cord. The majority of people with cervical SCI have tetraplegia that limits upper extremity function [1]. The restoration of hand and arm functions is the highest priority for people with cervical SCI [2], [3]. Although there are several on-going clinical studies, there are currently no effective therapeutic interventions for paralyzed hands and arms following SCI.

To restore function to paralyzed upper limbs, researchers have begun creating artificial connections between the brain and paralyzed limbs. These connections can be made by stimulating the muscles, their associated peripheral nerves, or the spinal cord below the injury [4]–[9]. Muscle and nerve stimulation can restore some function after SCI but requires individual controllers for separate target muscles or nerves. Muscle and nerve stimulation also leads to rapid muscle fatigue during stimulation, limiting their clinical adoption [10]–[12]. Alternatively, intraspinal micro-stimulation (ISMS) provides naturalistic recruitment of muscle fibers with functionally synergistic movement [13]–[16]. The clinical testing of ISMS, however, has proceeded slowly due to its invasiveness.

Epidural stimulation, an emerging alternative to ISMS, can produce evoked movements that are similar to ISMS [17], and is already approved for pain control in humans. Open-loop neuromodulation via epidural stimulation can lead to immediate functional gains in voluntary movements of the paralyzed upper limbs [18]. Brain controlled-epidural stimulation in animal models has also resulted in successful reanimation of arm and leg movements [19], [20]. Epidural stimulation triggered from limb movements has also shown promise in human trials [21].

Decoded movement intention from neural activity can be used to provide closed-loop control over stimulation of the

This work is licensed under a Creative Commons Attribution-NonCommercial-NoDerivatives 4.0 License.
For more information, see https://creativecommons.org/licenses/by-nc-nd/4.0/

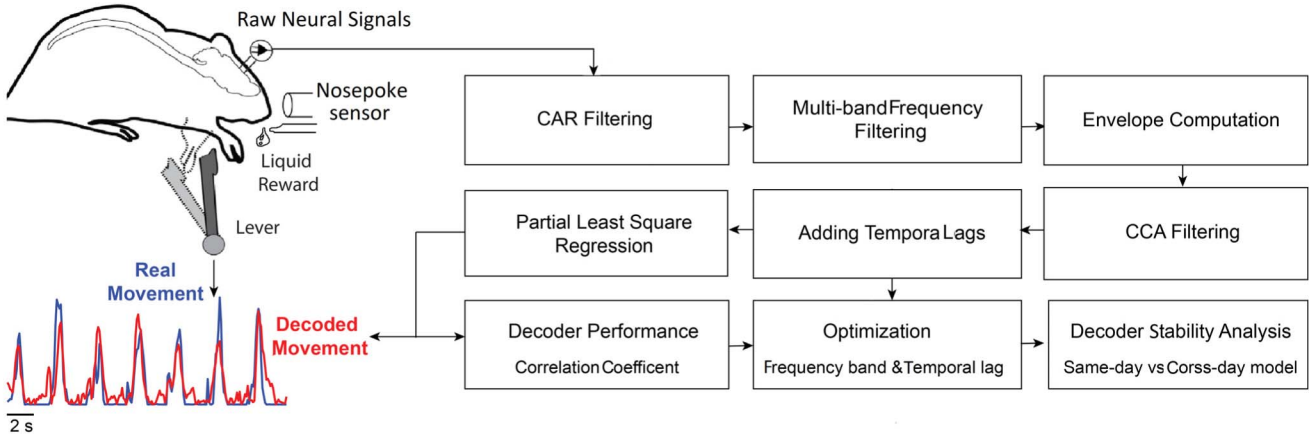

Fig. 1. **Offline pre-injury cortical decoding:** Raw neural signals were common average reference (CAR) -filtered to increase the signal-to-noise ratio of the recording. CAR filtered signals were bandpass filtered through different frequency bands. The power of each band was extracted using envelope computation. A canonical correlation analysis (CCA) filter was applied to each multi-channel envelope to capture the highest task-related activity from each frequency band. After combining CCA features, temporal lags from 0-300 ms were added to the feature space. Finally, a partial least square regression algorithm was applied on the spectro-temporal features to decode forelimb movement. The correlation coefficient between decoded movement and real lever movement was used as a metric for decoding accuracy. The single best frequency band and temporal lag was used to decrease the complexity of the final cortical decoder for online implementation (Optimization). Decoder stability was tested offline by evaluating the decoder performance in same-day and cross-day model conditions (Decoder Stability Analysis).

spinal cord or muscles. While several studies have demonstrated artificial connections between the brain and spinal cord [4], [7], [19], [20], decoding performance is often not stable over time. Computing methods of brain decoding must balance electrode invasiveness, limited hardware longevity, signal non-stationarities, and spatial resolution [22]–[24]. Single neuron action potentials, or spikes, have historically been used for neural decoding as they accurately predict intended movements [25]. Spike decoding additionally benefits from high spatiotemporal resolution [8], [9], [26]. Nevertheless, spike decoding has limited signal stability over days to weeks and requires frequent recalibration by researchers [27]. To overcome the limitations associated with spike-based decoding, we used intracortical local field potentials (LFPs). LFPs exhibit significantly increased signal stability over single-unit spikes while maintaining sufficient information to decode movement intention [28]. Furthermore, LFP decoders have lower bandwidth requirements than spikes, which translates to lower computational complexity of the decoder [29].

Here we investigated real-time control of epidural stimulation based on LFP decoding to restore functional movements after cervical SCI. We constructed a complete brain to spinal cord interface capable of decoding LFPs using a computationally efficient algorithm in order to control epidural stimulation. We tested whether the entire LFP decoding system can be implemented in a miniaturized implantable device that utilizes a field-programmable gate array (FPGA) to perform on-board processing [30]. Finally, we explored the feasibility of implementing the decoder to trigger epidural stimulation using the customized processing pipeline on a miniaturized device.

II. Methods

A. Animals

Eleven female Long Evans rats (250-360g) participated in this study and were trained on a novel lever pressing tasks (Fig. 1 Top Left). This included seven animals studied for the cortical decoding analysis with pre- and post-injury conditions (Fig. 1) and five animals using the brain-computer-spinal interface (BCSI) following SCI (Fig. 2). One animal was involved in both cortical decoding and BCSI system tests. All animal procedures were conducted in accordance with the National Institutes of Health guidelines for the care and use of experimental animals and were approved by the University of Washington Institutional Animal Care and Use Committee.

B. Experimental Overview

After animals underwent the behavior training and achieved task proficiency, animals were then implanted with intracortical micro-wires followed by a one-week recovery period. We conducted three offline decoding studies as follows (Fig. 1). First, we performed offline cortical decoding to assess decoding accuracy and optimize spectro-temporal features for forelimb movement decoding ($N = 7$). Second, we tested the stability of the decoder in the pre-injury condition ($N = 4$). In parallel, three of seven animals received a right lateralized C4 contusion injury and were tested for the accuracy of the decoding after injury ($N = 3$). To evaluate the closed-loop system in one animal from the previous cohort and four new animals, we implanted epidural electrodes over the right C6 spinal segment after the contusion injury ($N = 5$). Post-injury cortical decoding was performed to update the cortical decoder after SCI (Fig. 2). These five animals were then tested using the closed-loop system where cortically controlled spinal stimulation was used to complete the lever pressing task after injury.

C. Lever Task Training

A novel lever-pressing task was created to allow animals with a severely impaired forelimb to engage in the task while using the BCSI system. The behavior arena consisted of a translucent acrylic box with a gap on both sides of a central platform similar to the Montoya staircase [31]. A lever was positioned directly below the forelimb which was pressed backward by extending the elbow and shoulder. The starting lever position could be adjusted vertically and horizontally.

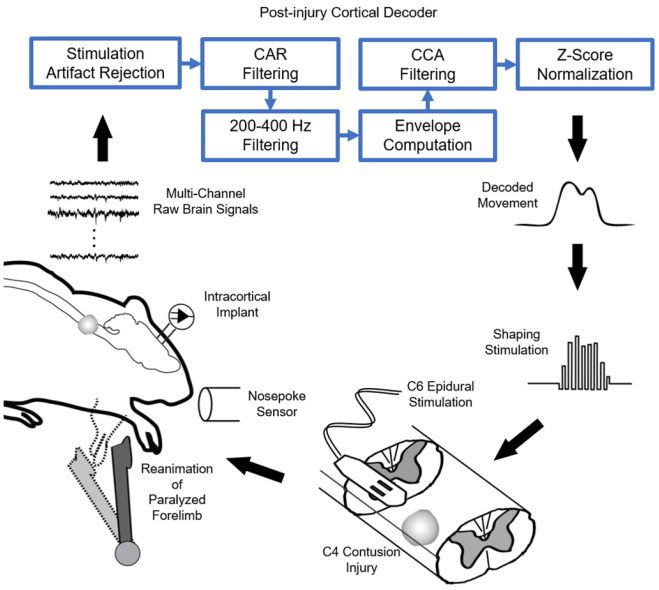

Fig. 2. **Design of Brain-Computer Spinal Interface system.** The decoder tuned via the offline analysis was used to decode animal intention to move after the injury. Stimulation artifacts were rejected using a sample-and-hold method. Multi-channel cortical signals were common reference average (CAR) filtered and band pass filtered to extract the high gamma frequency band (200-400 Hz). The power of each high-gamma LFP channel was obtained by envelope computation. The canonical correlation analysis (CCA) weights obtained from the post-injury cortical decoding modeling were used to decode movement. The decoded movement signal was z-score normalized and mapped to stimulation current amplitude. Stimulation was delivered via epidural electrodes implanted below the injury at spinal level C6, to reanimate forelimb movement after C4 contusion SCI. This restored forelimb and lever movement triggered the delivery of rewards.

A nose-poke sensor and a fluid reward tube were placed in front of the animal (Fig. 1 Top Left). The task involved placing the nose near the nose-poke sensor to keep the animals in a consistent position relative to the lever. The voluntary nose-poke additionally served to detect engagement with the task. To receive a reward, the rat had to reach and press the lever backward to a predetermined threshold while simultaneously remaining within the range of the nose-poke sensor. Animals were given an apple juice reward for successfully pressing the lever backward. Task training was performed five to twenty minutes each day, five days per week, for three to four weeks to achieve task proficiency. Proficiency was defined as completing at least 60 lever presses to maximum displacement within ten minutes. To increase motivation, the rats were water restricted between sessions. After each session, they were given one-hour unrestricted water access per day and free water during weekends.

D. Cortical Surgery

All surgeries were performed using sterile technique and 2-3% isoflurane anesthesia in oxygen. Body temperature was maintained at 37 °C using a heating pad during surgeries and recovery. Baytril (0.05 mg/kg) was administered pre-operatively. After a craniotomy and removal of the dura mater, custom-built 16-wire tungsten microelectrode arrays (8 × 2, 40 μm diameter, 200 μm space between adjacent wires) were inserted into the rostral and caudal forelimb area of the sensorimotor cortex. The 8 × 2 arrays were oriented with the long axis in the rostral-caudal direction. The middle of the implant was placed 1.5 mm rostral and 2.5 mm lateral to bregma and advanced 1.5 mm below the brain surface to record pyramidal neuron activity in layer V. The printed circuit board (PCB) connected to the cortical arrays was stabilized by dental cement on the skull. Buprenorphine (0.05 mg/kg) was administered twice per day for three days postoperatively.

E. Spinal Surgery

The contusion injury procedure began with a skin incision between the C2-T2 spinous processes and dissection of the muscle layers. Following a C4 unilateral laminectomy, we performed a right lateralized C4 contusion injury using by applying a 200 kdyn force using the Infinite Horizon Impactor (Precision Systems and Instrumentation, LLC., Fairfax Station, VA).

Epidural spinal stimulating electrodes were constructed as follows [32]. Two bundled electrode wires (0.27 mm diameter, 100 mm length, AS631, Cooner wire) were glued to a polyimide sheet (5 mm × 1.5 mm × 46 μm) using epoxy. Then, 1mm of Teflon Insulation was removed from each of the two wires. After a C7 unilateral laminectomy, the sterilized epidural implant was placed between the C5-C6 lamina and the dura mater from the caudal side of C6. Subsequently, the caudal side of the epidural implant was sutured to the dura over the dorsal aspect of the right C6 segment (7-0 Plypro, Surgipro II). A loop was formed near the spinal cord to provide strain relief. The wires were routed through a catheter to protect the stimulation wires (60 mm length, EC05500 Epidural Catheter, Arrow International). The catheter was anchored to the T2 spinous process with a 5-0 nylon suture for stability. A common ground wire was placed subcutaneously near the shoulder on the right forelimb. The stimulation wires and common ground were soldered to a printed circuit board for joining the wires to a connector. The printed circuit board was embedded in the headcap shared with the cortical implant.

F. Cortical and Behavioral Data Recording

Neural data were recorded using the TDT multi-channel data acquisition system at 24.4 kHz (Tucker-Davis Technologies, FL). The continuous lever press and nose-poke TTL signals were also recorded simultaneously via analog-to-digital ports. We collected at least 50 lever presses for each recording session. Both cortical and behavioral data were stored on a PC for further analyses.

G. Offline Pre-Injury Spectro-Temporal Feature Analysis

Offline analyses were performed to optimize forelimb movement decoding prior to online use with the BCSI system. The offline study was performed in MATLAB using custom scripts. We used the decoding paradigm presented in [33] to continuously decode forelimb movements from the multi-channel LFPs. Several preprocessing steps were implemented to remove artifacts/noise and improve decoding performance. We excluded channels with significant noise evident in their power spectral density as it indicated likely mechanical failure of the electrodes or connector. A common average reference (CAR) filter was used to increase the signal-to-noise ratio (SNR) of the recorded signal [34]. Finally, an outlier removal

algorithm was applied to cap particularly high voltages greater than three times the standard deviation of each LFP signal.

After artifact removal, all 16 channels were filtered into seven frequency sub-bands: δ (1-4 Hz), θ (4-8 Hz), α (8-12 Hz), β (12-30 Hz), $\gamma\,1$ (30-120 Hz), $\gamma\,2$ (120-200 Hz) and $\gamma\,3$ (200-400 Hz) using a 4^{th} order zero-lag Butterworth bandpass filter. Next, the envelope of each bandpass filtered signal was computed via rectification and a 4^{th} order zero-lag, 2.5 Hz low-pass Butterworth filter.

Movement-related features were extracted by applying a canonical correlation analysis (CCA) filter on the multi-channel envelopes of each frequency band. Applying CCA weights on different frequency bands produced seven CCA features, u(t). To decode movement at time t, CCA features were normalized to have zero mean and unit standard deviation. Temporal lags including u(t-0 ms), u(t-100 ms), u(t-200 ms), and u(t-300 ms) were calculated to produce a spectro-temporal feature matrix. Partial least squares regression (PLSR) was applied on the feature matrix to predict the forelimb movement vector, y(t). The correlation coefficient between the predicted and real signal was used to evaluate the accuracy of the decoder in the pre-injury condition. Decoder accuracy was evaluated using 5-fold cross-validation.

The best frequency band and temporal lag were chosen by evaluating decoding performance across all combinations. Specifically, decoders were constructed using a single frequency band and temporal lag. To compare the decoding performance of individual frequency bands and temporal lags, Friedman test followed by Bonferroni correction was applied on the correlation coefficient values obtained from four sessions from each in seven animals. This analysis revealed that the high gamma band was the best feature for movement decoding.

H. Offline Pre-Injury Cortical Decoding

Stability of the decoder and the underlying neural signals are both important factors for real-life brain-computer interface applications. Decoder stability was assessed by evaluating decoder performance across the entire study. Specifically, the performance was evaluated on decoders constructed from the best performing frequency band (200-400 Hz) and time lag (100 ms). Models trained on the first recording day (the cross-day model) were compared against models trained at the beginning of every session (the same-day model). In the same-day model condition, we created a movement decoder with training and testing data recorded in the same session. In the cross-day model condition, we trained a decoder with data from the first recording day and used that model on the remaining days. To compare the decoding accuracy between these two conditions, a Wilcoxon-signed ranked test was applied on correlation coefficient values obtained from the last session of each animal (4 sessions $*$ 5 folds $=$ 20 correlation coefficient values).

I. Offline Post-Injury Cortical Decoding

Following the contusion injury, the animals presented with severe right forelimb paresis (weakness). To study the ability of the multi-channel LFPs to predict forelimb movement after injury, we compared the modulation of high-gamma LFP features during forelimb movement between pre- and post-injury conditions. To quantify this modulation, we calculated the percent change of high-gamma LFP power from baseline (rest state) to the active period (movement state).

J. Online Brain-Controlled Spinal Stimulation

Five animals using the BCSI system were tested for online decoding and reanimation via epidural stimulation. Fig. 2 shows the schematic of the online forelimb movement decoder based on multi-channel LFPs. In the first step, the stimulation-induced artifacts after each stimulation pulse were removed. This artifact typically had a higher voltage amplitude than brain signals. We used a sample-and-hold algorithm to minimize the effect of this artifact on extracted features and consequently on the decoder. After each stimulation onset, we paused brain data sampling for 2 ms while holding the last sample at a fixed value. After removing the stimulation-induced artifact, we applied a common average reference (CAR) filter to increase the signal-to-noise ratio (SNR). Voltage amplitudes were constrained to three standard deviations of a baseline LFP signal recorded before each experiment. Suprathreshold signals were fixed at the respective upper and lower bounds.

To decrease the complexity of the cortical decoder for online implementation in future implanted hardware, the optimal frequency band and time lag were selected based on the prior offline analysis. Multi-channel cortical signals were filtered through these optimal frequency bands (200-400 Hz, 4^{th} order Butterworth). Bandpass filtered signals were rectified and smoothed (low pass filter, 4^{th} order Butterworth, 2.5 Hz) to obtain multi-channel envelopes. These envelopes were multiplied by corresponding CCA weights obtained from the training data to predict forelimb movements in real-time (Fig.2).

There is an inherent limitation in extracting the ground truth of movement intention in rats following SCI as they are unable to move their limbs. Instead, we used a signal based on an active nose-poke as a proxy for imagined or attempted movements, which have been successfully used to construct BCI decoders for human subjects with severe SCI [9], [10], [38], [39]. Therefore, to obtain CCA weights after injury, an artificial bell-shaped lever signal was inserted at time points where the nose-poke sensor was activated and immediately followed by residual lever press movement.

The decoded movement signal in the post-injury condition was z-score normalized before triggering the epidural stimulation. The normalization step was conducted based on 30 seconds of recorded cortical data at the beginning of each session. The normalized signal was mapped between the motor threshold and maximum stimulation amplitude to control epidural stimulation. Epidural stimulation was delivered whenever the decoded signal crossed a predetermined threshold while the animal simultaneously activated the nose-poke sensor (Fig. 3). This assured both a consistent body position and engagement with the task (Fig. 2).

The movement responses to the stimulus varied among animals due to the severity of injury and relative location of the epidural electrodes. Without stimulation, animals produced minimum lever press movement following C4 contusion injury (the Irvine, Beatties, and Bresnahan (IBB) scale: 1.6 $\pm$ 0.93

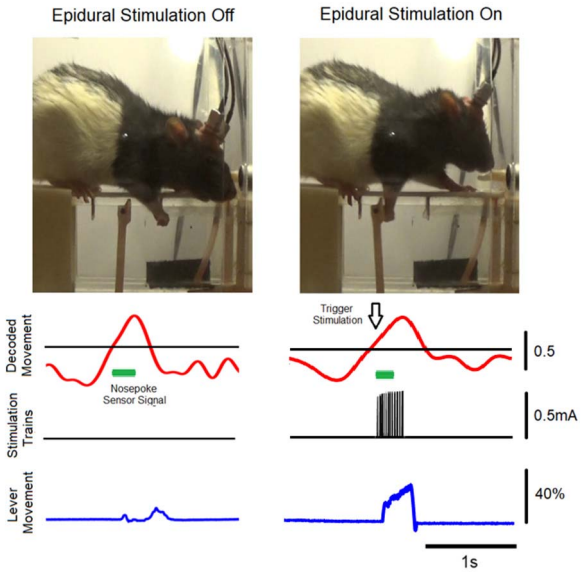

Fig. 3. **Brain-controlled stimulation protocol**. Based on the multichannel-LFPs, the lever movement was continuously decoded (red line). **Left**: Lever press performance with epidural stimulation Off in Animal #7 after the C4 contusion injury (Supplementary Video 2). The injured animal exhibits a limited lever press (blue line). **Right**: Online brain-controlled epidural stimulation On condition. The intracortical LFPs were used to decode movement. When the decoded lever movement stayed above a predefined threshold and the nose-poke sensor was activated (green line), stimulation was delivered to the spinal cord (Right, 2nd row). Stimulation via epidural electrodes at the C6 spinal segment evoked forelimb movements capable of moving the lever (Right, bottom row). Initially the decoded lever movement exceeded the threshold (black line), but the animal did not position their body correctly to activate the nose-poke sensor. The stimulation was triggered when the nose-poke sensor was activated (arrow). The decoded movement is presented as z-scores. The lever movement is normalized to maximum pre-injury lever displacement (%).

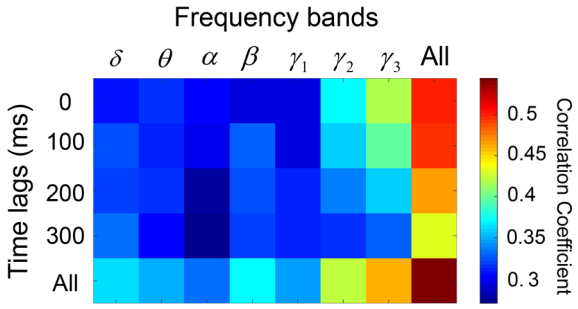

Fig. 4. **Contribution of separate frequency sub-bands and temporal lags to movement decoding.** All data were obtained from the pre-injury condition. Frequency sub-bands are δ (1-4 Hz), θ (4-8 Hz), α (8-12 Hz), β (12-30 Hz), γ1 (30-120 Hz), γ2 (120-200 Hz) and γ3 (200-400 Hz). Positive lags indicate that the neural data occurs before the behavior. Each color shows the mean correlation coefficients for N = 7 animals. Considering all frequency and all-time lags leads to highest decoding performance. When limited to a single frequency band and time lag, however, the frequency band of γ3 (200-400 Hz) and time lag of 100 ms produced the best decoding performance.

(mean ± SEM), N = 5, 40-60 days post-injury) [35]. Based on stimulation responses in each animal, we determined the number of pulses and burst frequency at the beginning of the recording sessions needed to restore a robust lever pressing movement. We used charge-balanced biphasic square-wave pulses with 400μs pulse width delivered in 15-40 pulse trains at 50-100 Hz (Model 2200, A-M systems). We scaled the starting stimulation current amplitude to evoke elbow extension movement in each experiment (300μA-1mA).

K. Functional Assessment

The range of lever motion was measured to quantify the performance of the BCSI system for movement restoration. Catch trials with stimulation off were randomly interleaved at 20-30% probability. Lever movement was compared between the stimulation on condition (BCSI On) and the Catch trial without spinal stimulation in the same session. As an additional metric to quantify the functional behavior, we used the reward rate to capture the efficiency of lever press performance. Reward rate was defined as the number of successful lever presses and thus rewards per minute in 2-4 minute blocks of BCSI On and Catch trials.

L. Miniaturized BCSI System

The miniaturized BCSI system was tested offline using a modular field-programmable gate array (FPGA)-based device, modified from our Neural Closed-Loop Implantable Platform (NeuralCLIP) [30]. This miniaturized electronic device could record cortical signals, process multi-channel LFP data, and decode movement intention to trigger stimulation.

The structure of the miniaturized BCSI hardware consisted of the Intan Technologies RHS2116 microchip (Los Angeles, CA) for recording and stimulation. The Intan chip contains 16 channels and a 16-bit ADC controlled by a serial peripheral interface (SPI) and was coupled to a low-power FPGA (AGLN250, Microsemi, Aliso Viejo, CA).

The miniaturized BCSI device used approximate computing blocks to perform different parallel tasks to decode forelimb movement from multi-channel LFPs, including multi-channel bandpass filtering, CAR filtering, rectification, signal smoothing, downsampling, and CCA weight multiplication. To evaluate the utility of the miniaturized BCSI system, prerecorded brain signals from both pre- and post-SCI animals were provided as inputs to the miniaturized BCSI. The predetermined CCA weights were updated on the FPGA prior to signal processing. The signals were processed through the data pipeline located on the FPGA to predict stimulation timing.

M. Statistical Procedures

All data are reported as mean ± SEM. All data were assessed for normality with the Kolmogorov–Smirnov test. None of the data collected for statistical analysis were normally distributed. Friedman test accompanied by Bonferroni correction was used to test for significant difference between multi-band frequencies or temporal lags. A non-parametric Wilcoxon signed-rank test was used for the decoder stability analysis and lever press efficiency performance assessment with and without the BCSI On. Moreover, lever press ranges with and without the BCSI On were evaluated using the Wilcoxon rank-sum to allow for differences in the total number of lever presses in each condition from all animals. All analyses were performed with SPSS software Version 25 (Chicago, IL). Differences were considered significant at p-value < 0.05.

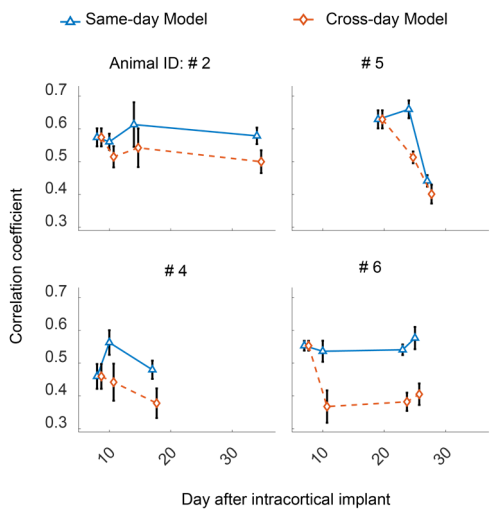

Fig. 5. **Long term stability of forelimb movement decoder.** Stability of forelimb movement decoding with the high gamma LFP feature was compared between models trained on the same day and models trained only on the first experimental session. Each data point is the mean ± SEM correlation coefficient (R-value) of the test set obtained from 5-fold cross-validation. Same-day calibration of the decoder produced marginally better decoding accuracy compared to the cross-day model. Even without same-day calibration, however, the LFP-based decoder could still produce sufficient decoding performance for up to 30 days. Each panel depicts data from one of four animals.

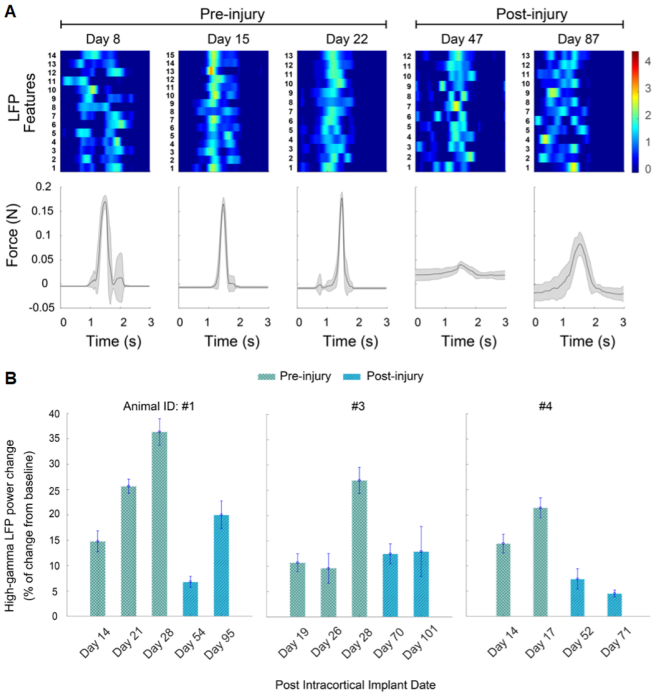

Fig. 6. **Sustained LFP power in pre- and post-injury conditions.** **A:** Average multi-channel 200-400 Hz LFP features were aligned with lever presses across many days after intracortical array implantation. In both pre- and post-injury conditions the high gamma LFP power in multiple channels increased before the lever press and during holding of the lever, followed by a decrease to baseline when the animal released the lever. **B:** Each bar shows the high gamma LFP power change during movement from the baseline activity during rest periods averaged over all trials in each session (mean ± SEM). This demonstrates that lever movement could be decoded for 71-101 days in each animal despite a spinal cord injury occurring at the midpoint of the experiment.

III. Results

A. Offline Pre-Injury Cortical Decoding

We analyzed the contribution of spectral and temporal LFP information, as well as the stability of the forelimb movement decoder, with the goal of developing a stable and computationally efficient brain-computer-spinal interface.

First, we evaluated the movement decoding accuracy of different frequency bands and temporal lags. Fig. 4 compares decoding performance of individual frequency bands and time lags. Each color shows the mean of the correlation coefficient obtained from four sessions each in seven animals using 5-fold cross-validation. As we expected, including all frequency bands leads to the highest decoding accuracy. There was not, however, a significant reduction in decoding accuracy when using just the 200-400 Hz high gamma band compared to combining all frequency bands ($p = 0.09$, Friedman test with Bonferroni correction). In addition, decoding using only the 200-400 Hz (γ 3) frequencies outperformed all other individual frequency bands ($p < 0.01$). The LFP decoder with high gamma bands consistently produced predictions that were highly correlated with the real lever trajectory and were comparable to previous studies [27], [36].

Including all temporal lags from 0-300 ms produced the highest decoding accuracy, which was significantly greater compared to individual time lags ($p < 0.001$, Friedman test with Bonferroni correction). When using a single time lag, 100 ms lags resulted in significantly better decoding performances compared to 200 ms and 300 ms lags ($p < 0.05$). It should be noted that the use of a low pass filter for envelope extraction may result in some of the extracted features appearing in more than one-time bin.

To evaluate the stability of the decoding model with high gamma frequency band (200-400 Hz) and time lag (100ms), we assessed the decoder performance across the entire study using two conditions. In the first condition, the decoder was trained and tested using data from the same day (same-day model) across all sessions. In the second condition, the cortical decoder was trained on the first session and then tested on the following days (cross-day model). Decoding accuracy was assessed by the correlation coefficient between real and predicted movement with 5-fold cross-validation. Fig. 5 shows the decoding accuracy of the movement for the same-day and cross-day models. Using the same-day model leads to significantly better decoding performance in comparison to the cross-day model (N = 4, $p = 0.03$, one-tailed Wilcoxon signed-rank test). Nevertheless, the average correlation coefficient of the cross-day model remained above 0.35 in four animals for more than one month. This level of decoding performance was sufficient to identify different states of movement, such as lever press and lever release even without recalibration.

We found little correlation between nose-poke activation and multi-channel cortical information (correlation coefficient = 0.06 ± 0.1, mean ± std, N = 7). By contrast, the correlation between lever movement and multi-channel cortical signals was significantly higher (correlation coefficient = 0.47 ± 0.1, N = 7 $p < 0.0001$; one-tailed Wilcoxon signed-rank test). This indicates that we were decoding the intention to produce upper limb movement rather than

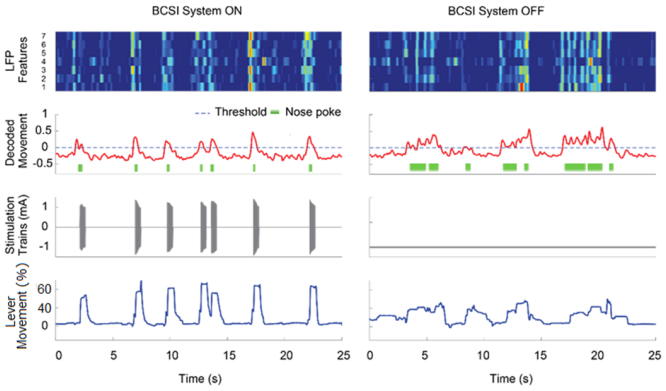

Fig. 7. **Operation of the BCSI system. Left:** Stimulation On trials. Animal #3 performed the lever task with LFP-controlled epidural stimulation. Each band on the top row represents a channel of high gamma LFP power. During the intended movement, the power of the high gamma band increased in the majority of channels. **Right:** Catch trials. During the stimulation Off period, the animal still demonstrated periodic high gamma power increases correlated with nose-poke behavior (green raster) indicating intention to press the lever. Lever movement is shown as a percentage of the pre-injury function.

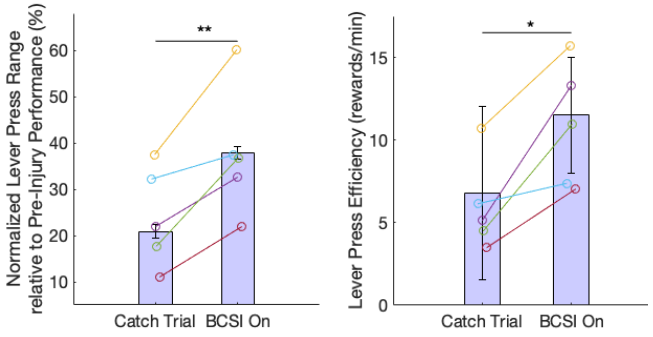

Fig. 8. **BCSI system improved forelimb function. Left:** Average reanimated forelimb movement by the brain-computer spinal interface (BCSI) was significantly greater compared to the stimulation off catch trials (N = 5 animals, Catch Trial total 168 presses, BCSI On total 159 presses; ** p-value < 0.001, Wilcoxon rank-sum test). **Right:** The mean number of rewards per minutes also significantly improved when using the BCSI compared to the catch trials (Catch Trial total 17 blocks and BCSI On total 17 blocks in five animals; * p-value = 0.0023, Wilcoxon signed-rank test). Data points show average lever press performance in each animal.

the body position or movements used to activate the nose-poke sensor.

B. Offline Post-Injury Cortical Decoding

The stability of the decoder is also critical after injury. Therefore, we tested the performance of the decoder created in the pre-injury offline analysis for use in animals following injury. Fig. 6 A shows an example of the modulations in high-gamma LFP power during movement and rest in pre- and post-injury conditions. Even after the injury, high-gamma LFP power was modulated during the lever presses. Fig. 6 B shows that this modulation continues across more than 70 days in multiple animals. This indicates that the high-gamma LFP feature is a suitable feature for decoding movement intention even after injury. Next, we implemented this high-gamma LFP decoder in the BCSI system to control cervical epidural stimulation.

C. Brain-Controlled Spinal Stimulation for Reanimation

To demonstrate an application of the high-gamma LFP decoder, we tested whether the closed-loop BCSI could improve paralyzed forelimb function following severe cervical SCI in freely moving rats. Intracortical LFPs were used to decode the animals' intention to move. The decoder triggered epidural stimulation, which was delivered to the lateral C6 vertebral spinal cord to produce forelimb extension movement (Fig. 7 Left; Supplementary Video 1 & 2). In Catch trials, the stimulation was briefly turned off to assess lever press performance in the absence of stimulation. When the stimulator was off, the animals struggled to press the lever and failed to reach the reward threshold (Fig. 7 Right). Despite failing to perform the task, movement intention was still visible as increased activity in the decoded movement aligned with nose-poke sensor activation. Nose-poke sensor activation was a trained behavioral response that was required during performance of the lever press to keep the animal's body in position.

D. Functional Improvement With BCSI

All five animals were able to use the BCSI system after the injury to improve their forelimb function. To quantify the improvement in forelimb function, we compared the post-injury peak lever range using the BCSI system (BCSI On Trials) and without stimulation (Catch Trials). Average reanimated forelimb movement by the BCSI was significantly greater (38 $\pm$ 1%) than the stimulation off post-injury trials (21 $\pm$ 2%, $p < 0.001$, Wilcoxon rank-sum test; Fig. 8 Left). Second, we quantified the efficiency of lever press performance in the testing sessions. The average number of rewards per minute with the BCSI On condition was significantly greater (11.5 $\pm$ 3.5 rewards/min) than the performance in the catch trials (6.8 $\pm$ 5.2 rewards/min, p = 0.0023, Wilcoxon signed-rank test; Fig. 8 Right).

E. Autonomous BCSI Miniaturized Device

Finally, we evaluated the performance of the autonomous decoding system on the NeuralCLIP. The NeuralCLIP was configured with signal processing blocks to implement our CCA decoder on an FPGA architecture [30]. The complete system was implemented on a PCB small enough to be implanted under the skin of a rodent. To test the NeuralCLIP's ability to perform the necessary signal processing blocks, prerecorded neural data from both before and after injury were used as inputs to the onboard FPGA. To improve detection of movement intention from the previous work [30], a rectifying block was placed between the bandpass filter and CCA. A downsampler followed by a smoothing filter was placed after the CCA output to improve threshold detection for decoded movement (Fig. 9a). The refined NeuralCLIP could detect the lever press movement intention from the LFPs and predicted the timing of the real lever movement in the uninjured condition (Fig. 9b) as well as the nose-poke signals as a proxy for lever movement in the injured condition (Fig. 9c). These results suggest that a computationally efficient decoder can run on an implantable device and provide the

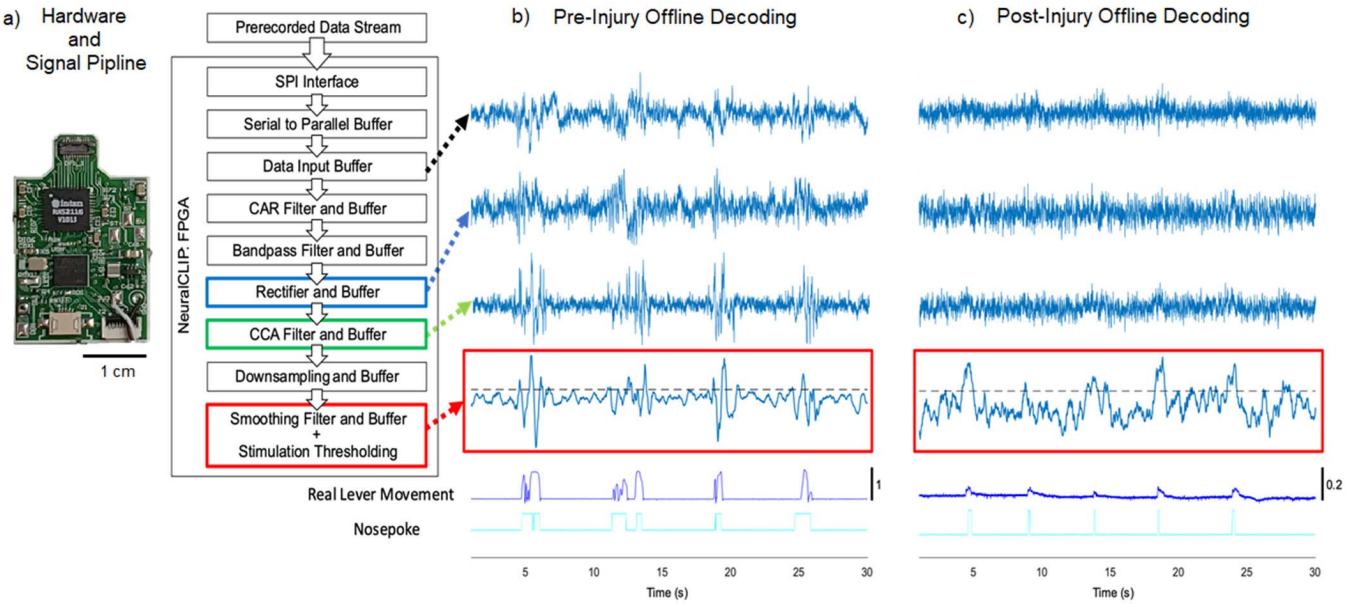

Fig. 9. **Autonomous miniaturized platform decoded movement intention to trigger stimulation pre- and post-injury a)** Hardware and Pipeline Blocks of the Neural Closed-Loop Implantable Platform (NeuralCLIP: **Left**), which processed pre-recorded LFP signals from the motor cortex and identified events to trigger stimulation. The block diagram demonstrates the processing pipeline (**Right**). Modifications from the original NeuralCLIP pipeline include a rectifier, downsampler and smoothing filter to improve the decoding performance while maintaining low power consumption. **b) & c)** Offline Decoding of Lever Movement in Pre- and Post-injury Condition. The CCA-decoded lever movement was calculated from 4 cortical channels. The first row shows one channel of raw brain signal input. The second row shows the rectified single channel signal after processing by a common average reference (CAR) filter and a 200-400Hz band-pass filter. The third row illustrates the multichannel CCA filtered signal. After down sampling and smoothing, the decoded lever movement (red box) could trigger stimulation by crossing a pre-determined threshold (dashed line). The decoded movement is aligned with the actual lever movement and nosepoke signals (bottom). The NeuralCLIP successfully decoded forelimb movement intention with the pre-recorded brain signals recorded in both pre- and post-injury conditions in this example animal.

necessary processing to control spinal stimulation and promote simple functional restoration after spinal cord injury.

IV. Discussion

Here we demonstrate a brain-computer-spinal interface (BCSI) for restoring functional upper limb movement following cervical spinal cord injury. Our main findings are: 1) intracortical high gamma local field potentials provide a stable marker of forelimb movement intention without recalibration over many days before and after spinal cord injury, 2) brain-controlled epidural stimulation improves forelimb function, and 3) the computationally efficient closed-loop algorithm can be implemented on a miniaturized device with onboard computing. Both the recording and stimulation techniques used here have already been used separately in human clinical trials. By combining these techniques in the present study, our results inform a pathway to the clinical translation of BCSI technology to humans.

A. Local Field Potential Decoding

We found that the high gamma LFP decoder provided accurate and stable predictions of forelimb movement trajectory over time. LFPs reflect the summation of multiple neural sources near the recording area [37]. Previous studies confirmed that both multiunit spike activity and LFPs allow accurate prediction of movement related information [28]. A prior study reported similar decoding performance using LFP activity compared to multiunit spikes due to greater signal stability of LFPs in non-human primates [38]. LFP decoders have also shown sufficient stability for motor intention decoding without recalibration over several months in human subjects [39]. In prior work, the CCA decoder used here maintained high performance with a lower computational complexity compared to principal component analysis or correlation coefficient-based methods [33].

In the present study, we demonstrated that the frequency band between 200-400 Hz provided the highest accuracy for decoding forelimb lever press movement compared to other isolated frequency bands. Using the CCA decoder on multichannel LFPs in the 200-400 Hz band, we demonstrated accurate and stable decoding over many days, similar to a previous study in non-human primates [38]. This is a substantial advantage over spike-based decoders that often require daily spike sorting procedures and frequent refitting [8], [9].

An additional benefit of using a CCA with a single LFP frequency band is reduced computational complexity. Despite the limited spatial resolution of LFPs, the increased computational efficiency of the proposed decoding strategy allowed us to implement the complete closed-loop system on a miniature device small enough to be implantable. Similar strategies may accelerate clinical translation of closed-loop BCI systems by eliminating the need for percutaneous cabling or high bandwidth wireless data transfer [40]. To accomplish this, we selected a clinically viable stimulation strategy to be controlled by the output of the CCA decoder for upper limb reanimation.

B. Epidural Stimulation for Upper Limb Reanimation

Upper limb movements are less rhythmic with more supraspinal control compared to lower extremity tasks such as

walking [41]. Current BCI applications controlling functional muscle stimulation require a large number of stimulation electrodes [42]. Direct muscle or peripheral nerve stimulation can provide functional gains [8], [9] but evoke non-physiological recruitment of muscle fibers leading to rapid muscle fatigue [43]. One solution to fatigue is stimulation of the spinal cord, such as intraspinal microstimulation (ISMS), which provides a more natural recruitment order [13], [14], [44]. Here we extend these findings to epidural stimulation and demonstrate a functional forelimb extension movement. Even our simple LFP decoder-controlled epidural stimulation system could improve the outcomes of the multi-joint lever pressing task. Further experiments are required to investigate effective stimulation protocols to evoke graded forelimb movement via epidural stimulation, with a task that requires continuous modulation proportional to the cortical activity.

C. Hardware Application

Current BCIs require external desktops or tablet computers for decoding and control of stimulation or actuators [20], [45]. Even though some BCI systems are wireless, an external device is still necessary [46]. This limits the use of the BCI systems outside of research laboratories and presents challenges to translation, home use, or community applications. Onboard computing on implantable systems is one solution. However, the computational power on the implant is limited due to heat dissipation with current technology. Onboard computing also reduces the latency of communication to and from an external computer.

We previously presented the NeuralCLIP, a modular FPGA-based device (Fig. 9a) that can provide scalable, autonomous processing and stimulation in a size appropriate for untethered animal use or implantation [30]. In the present study, we added extra processing steps to our previous work to enable LFP decoding and stimulation control. This was needed because the modulation of LFP power was less robust in the animal with SCI than in the pre-injury condition (Fig. 9c). The CCA-based algorithm for LFP decoding was successfully implemented on the autonomous FPGA and triggered stimulation based on neural data recorded both before and after the injury.

Furthermore, the power consumption was on the order of 10 mW [30] which can be provided by wireless power transmission [47]. Wireless power transmission eliminates the need for large batteries and moves the BCSI system closer to an implantable form-factor. We have not yet performed an *in-vivo* study with this implantable system, as further research is needed to confirm if heat dissipation from the wireless power receiver is safe for surrounding tissue.

D. Limitations

In the offline study, we used zero-lag filtering techniques to analyze the decoder. For online implementation, however, we used a 4th order Butterworth that produced a 4 ms temporal delay given a 1 kHz sampling rate. This brief delay, however, is acceptable for closed-loop control of neural interfaces [48].

Restoration of daily activity using the paralyzed arms and hands requires movement with multiple degrees of freedom (DOF). This study required animals to perform only a one DOF movement. It is likely that LFPs contain the information for at least three-dimensional movement of the arm and hand [49]. Future work is needed to adapt decoding strategies that can extract multi-dimensional movement with low power consumption.

Although we demonstrated accurate LFP decoding using prerecorded signals to trigger stimulation on the miniaturized system, actual stimulation was not produced by the NeuralCLIP. One goal of this study was to test our ability to replace the external computers that were otherwise used for closing the loop. In future experiments, the device can be configured through SPI to stimulate in response to decoder output in real-time applications.

Using epidural stimulation to increase the variety of forelimb movements may require a wider implant with a larger number of channels to cover multiple spinal segments and dorsal root entry zones [50]. This requires advancements in electrode technology that are already underway [51] and also an increased physiological understanding of spinal cord stimulation [52], [53].

V. Conclusion

We found that brain-controlled epidural stimulation restored volitional control of a paretic forelimb in rats with severe cervical SCI. The computationally efficient algorithm connects clinically applicable recording and stimulation methods enabling implementation on a miniaturized autonomous closed-loop system. Thus, the BCSI strategy demonstrated here may overcome several barriers to translating BCIs into clinical approaches for upper limb restoration following SCI.

Acknowledgment

The authors thank A.M.V. Ievins for the initial support for the experimental design and A. Fischedick for animal care and training.

References

[1] *Spinal Cord Injury Facts and Figures at a Glance*, NSCISC, Univ. Alabama Birmingham, Birmingham, U.K., 2019.
[2] K. D. Anderson, "Targeting recovery: Priorities of the spinal cord-injured population," *J Neurotrauma*, vol. 21, no. 10, pp. 1371–1383, Oct. 2004.
[3] J. S. French *et al.*, "What do spinal cord injury consumers want? A review of spinal cord injury consumer priorities and neuroprosthesis from the 2008 neural interfaces conference," *Neuromodulation*, vol. 13, no. 3, pp. 229–231, Jul. 2010.
[4] J. B. Zimmermann and A. Jackson, "Closed-loop control of spinal cord stimulation to restore hand function after paralysis," *Frontiers Neurosci.*, vol. 8, p. 87, May 2014.
[5] C. Ethier *et al.*, "Restoration of grasp following paralysis through brain-controlled stimulation of muscles," *Nature*, vol. 485, no. 7398, pp. 368–371, May 2012.
[6] C. T. Moritz, S. I. Perlmutter, and E. E. Fetz, "Direct control of paralysed muscles by cortical neurons," *Nature*, vol. 456, no. 7222, pp. 639–642, Dec. 2008.
[7] Y. Nishimura, S. I. Perlmutter, and E. E. Fetz, "Restoration of upper limb movement via artificial corticospinal and musculospinal connections in a monkey with spinal cord injury," *Frontiers Neural Circuits*, vol. 7, p. 57, Apr. 2013.
[8] C. E. Bouton *et al.*, "Restoring cortical control of functional movement in a human with quadriplegia," *Nature*, vol. 533, no. 7602, pp. 247–250, May 2016.
[9] A. B. Ajiboye *et al.*, "Restoration of reaching and grasping movements through brain-controlled muscle stimulation in a person with tetraplegia: A proof-of-concept demonstration," *Lancet*, vol. 389, no. 10081, pp. 1821–1830, May 2017.

[10] R. M. Enoka and J. Duchateau, "Muscle fatigue: What, why and how it influences muscle function," *J. Physiol.*, vol. 586, no. 1, pp. 11–23, Jan. 2008.

[11] H. Kern *et al.*, "Denervated muscles in humans: Limitations and problems of currently used functional electrical stimulation training protocols," *Artif. Organs*, vol. 26, no. 3, pp. 216–218, Mar. 2002.

[12] N. Bhadra and P. H. Peckham, "Peripheral nerve stimulation for restoration of motor function," *J. Clin. Neurophysiol.*, vol. 14, no. 5, pp. 378–393, Sep. 1997.

[13] V. K. Mushahwar and K. W. Horch, "Selective activation and graded recruitment of functional muscle groups through spinal cord stimulation," *Ann. New York Acad. Sci.*, vol. 860, pp. 531–535, Nov. 1998.

[14] J. A. Bamford, C. T. Putman, and V. K. Mushahwar, "Intraspinal microstimulation preferentially recruits fatigue-resistant muscle fibres and generates gradual force in rat," *J. Physiol.*, vol. 569, no. 3, pp. 873–884, Dec. 2005.

[15] C. T. Moritz, T. H. Lucas, S. I. Perlmutter, and E. E. Fetz, "Forelimb movements and muscle responses evoked by microstimulation of cervical spinal cord in sedated monkeys," *J. Neurophysiol.*, vol. 97, no. 1, pp. 110–120, Jan. 2007.

[16] J. B. Zimmermann, K. Seki, and A. Jackson, "Reanimating the arm and hand with intraspinal microstimulation," *J. Neural Eng.*, vol. 8, no. 5, Oct. 2011, Art. no. 054001.

[17] C. Tao *et al.*, "Comparative study of intraspinal microstimulation and epidural spinal cord stimulation," in *Proc. Conf. IEEE Eng. Med. Biol. Soc.*, Jul. 2019, pp. 3795–3798.

[18] D. C. Lu *et al.*, "Engaging cervical spinal cord networks to reenable volitional control of hand function in tetraplegic patients," *Neurorehabilitation Neural Repair*, vol. 30, no. 10, pp. 951–962, Nov. 2016.

[19] M. Bonizzato *et al.*, "Brain-controlled modulation of spinal circuits improves recovery from spinal cord injury," *Nature Commun.*, vol. 9, no. 1, p. 3015, Aug. 2018.

[20] S. Micera *et al.*, "A brain-spine interface alleviating gait deficits after spinal cord injury in primates," *Nature*, vol. 539, no. 7628, pp. 284–288, 2016.

[21] F. B. Wagner *et al.*, "Targeted neurotechnology restores walking in humans with spinal cord injury," *Nature*, vol. 563, no. 7729, pp. 65–71, 2018.

[22] J. C. Barrese *et al.*, "Failure mode analysis of silicon-based intracortical microelectrode arrays in non-human primates," *J. Neural Eng.*, vol. 10, no. 6, Dec. 2013, Art. no. 066014.

[23] J. D. Simeral, S.-P. Kim, M. J. Black, J. P. Donoghue, and L. R. Hochberg, "Neural control of cursor trajectory and click by a human with tetraplegia 1000 days after implant of an intracortical microelectrode array," *J. Neural Eng.*, vol. 8, no. 2, Apr. 2011, Art. no. 025027.

[24] A. Campbell and C. Wu, "Chronically implanted intracranial electrodes: Tissue reaction and electrical changes," *Micromachines*, vol. 9, no. 9, p. 430, Aug. 2018.

[25] D. M. Brandman, S. S. Cash, and L. R. Hochberg, "Review: Human intracortical recording and neural decoding for brain–computer interfaces," *IEEE Trans. Neural Syst. Rehabil. Eng.*, vol. 25, no. 10, pp. 1687–1696, Oct. 2017.

[26] A. K. Bansal, W. Truccolo, C. E. Vargas-Irwin, and J. P. Donoghue, "Decoding 3D reach and grasp from hybrid signals in motor and premotor cortices: Spikes, multiunit activity, and local field potentials," *J. Neurophysiol.*, vol. 107, no. 5, pp. 1337–1355, Mar. 2012.

[27] J. A. Perge *et al.*, "Reliability of directional information in unsorted spikes and local field potentials recorded in human motor cortex," *J. Neural Eng.*, vol. 11, no. 4, 2014, Art. no. 046007.

[28] R. D. Flint, Z. A. Wright, M. R. Scheid, and M. W. Slutzky, "Long term, stable brain machine interface performance using local field potentials and multiunit spikes," *J. Neural Eng.*, vol. 10, no. 5, Oct. 2013, Art. no. 056005.

[29] M. W. Slutzky, "Brain-machine interfaces: Powerful tools for clinical treatment and neuroscientific investigations," *Neuroscientist*, vol. 25, no. 2, 2018, Art. no. 1073858418775355.

[30] V. Ranganathan *et al.*, "NeuralCLIP: A modular FPGA-based neural interface for closed-loop operation," in *Proc. 9th Int. IEEE/EMBS Conf. Neural Eng. (NER)*, Mar. 2019, pp. 791–794.

[31] C. Montoya, L. J. Campbell-Hope, K. D. Pemberton, and S. B. Dunnett, "The 'staircase test': A measure of independent forelimb reaching and grasping abilities in rats," *J. Neurosci. Methods*, vol. 36, nos. 2–3, pp. 219–228, 1991.

[32] M. Alam *et al.*, "Electrical neuromodulation of the cervical spinal cord facilitates forelimb skilled function recovery in spinal cord injured rats," *Experim. Neurol.*, vol. 291, pp. 141–150, May 2017.

[33] A. Khorasani, R. Foodeh, V. Shalchyan, and M. R. Daliri, "Brain control of an external device by extracting the highest force-related contents of local field potentials in freely moving rats," *IEEE Trans. Neural Syst. Rehabil. Eng.*, vol. 26, no. 1, pp. 18–25, Jan. 2018.

[34] K. A. Ludwig, R. M. Miriani, N. B. Langhals, M. D. Joseph, D. J. Anderson, and D. R. Kipke, "Using a common average reference to improve cortical neuron recordings from microelectrode arrays," *J. Neurophysiol.*, vol. 101, no. 3, pp. 1679–1689, Mar. 2009.

[35] K.-A. Irvine *et al.*, "The irvine, beatties, and bresnahan (IBB) forelimb recovery scale: An assessment of reliability and validity," *Frontiers Neurol.*, vol. 5, p. 116, Jul. 2014.

[36] M. W. Slutzky, L. R. Jordan, E. W. Lindberg, K. E. Lindsay, and L. E. Miller, "Decoding the rat forelimb movement direction from epidural and intracortical field potentials," *J. Neural Eng.*, vol. 8, no. 3, Jun. 2011, Art. no. 036013.

[37] G. Buzsaki, C. A. Anastassiou, and C. Koch, "The origin of extracellular fields and currents—EEG, ECoG, LFP and spikes," *Nature Rev. Neurosci.*, vol. 13, no. 6, pp. 407–420, May 2012.

[38] R. D. Flint, M. R. Scheid, Z. A. Wright, S. A. Solla, and M. W. Slutzky, "Long-term stability of motor cortical activity: Implications for brain machine interfaces and optimal feedback control," *J. Neurosci.*, vol. 36, no. 12, pp. 3623–3632, Mar. 2016.

[39] T. Milekovic *et al.*, "Stable long-term BCI-enabled communication in ALS and locked-in syndrome using LFP signals," *J. Neurophysiol.*, vol. 120, no. 1, pp. 343–360, Jul. 2018.

[40] R. Das, F. Moradi, and H. Heidari, "Biointegrated and wirelessly powered implantable brain devices: A review," *IEEE Trans. Biomed. Circuits Syst.*, vol. 14, no. 2, pp. 343–358, Apr. 2020.

[41] V. Dietz and K. Fouad, "Restoration of sensorimotor functions after spinal cord injury," *Brain*, vol. 137, no. 3, pp. 654–667, Mar. 2014.

[42] B. Wodlinger, J. E. Downey, E. C. Tyler-Kabara, A. B. Schwartz, M. L. Boninger, and J. L. Collinger, "Ten-dimensional anthropomorphic arm control in a human brain-machine interface: Difficulties, solutions, and limitations," *J. Neural Eng.*, vol. 12, no. 1, Feb. 2015, Art. no. 016011.

[43] R. Merletti, M. Knaflitz, and C. J. De Luca, "Myoelectric manifestations of fatigue in voluntary and electrically elicited contractions," *J. Appl. Physiol.*, vol. 69, no. 5, pp. 1810–1820, Nov. 1990.

[44] B. J. Holinski *et al.*, "Intraspinal microstimulation produces over-ground walking in anesthetized cats," *J. Neural Eng.*, vol. 13, no. 5, Oct. 2016, Art. no. 056016.

[45] J. M. Weiss, R. A. Gaunt, R. Franklin, M. L. Boninger, and J. L. Collinger, "Demonstration of a portable intracortical brain-computer interface," *Brain-Comput. Interfaces*, vol. 6, no. 4, pp. 106–117, Oct. 2019.

[46] C. Zickler, S. Halder, S. C. Kleih, C. Herbert, and A. Kübler, "Brain painting: Usability testing according to the user-centered design in end users with severe motor paralysis," *Artif. Intell. Med.*, vol. 59, no. 2, pp. 99–110, Oct. 2013.

[47] L. Arjona, J. Rosenthal, J. R. Smith, and C. T. Moritz, "High performance flexible protocol for backscattered-based neural implants," in *Proc. IEEE-APS Top. Conf. Antennas Propag. Wireless Commun. (APWC)*, Sep. 2019, pp. 276–280.

[48] J. M. Carmena *et al.*, "Learning to control a brain–machine interface for reaching and grasping by primates," *PLoS Biol.*, vol. 1, no. 2, p. e42, Oct. 2003.

[49] A. Jackson and T. M. Hall, "Decoding local field potentials for neural interfaces," *IEEE Trans. Neural Syst. Rehabil. Eng.*, vol. 25, no. 10, pp. 1705–1714, Oct. 2017.

[50] N. Greiner *et al.*, "Recruitment of upper-limb motoneurons with epidural electrical stimulation of the cervical spinal cord," *Nature Commun.*, vol. 12, no. 1, p. 435, Jan. 2021.

[51] G. Schiavone *et al.*, "Soft, implantable bioelectronic interfaces for translational research," *Adv. Mater.*, vol. 32, no. 17, Apr. 2020, Art. no. 1906512.

[52] M. D. Sunshine, F. S. Cho, D. R. Lockwood, A. S. Fechko, M. R. Kasten, and C. T. Moritz, "Cervical intraspinal microstimulation evokes robust forelimb movements before and after injury," *J. Neural Eng.*, vol. 10, no. 3, Jun. 2013, Art. no. 036001.

[53] M. Alam *et al.*, "Electrical neuromodulation of the cervical spinal cord facilitates forelimb skilled function recovery in spinal cord injured rats," *Experim. Neurol.*, vol. 291, pp. 141–150, May 2017.